UC Irvine
UC Irvine Previously Published Works

Title
The impacts and implications of an intensifying fire regime on Alaskan boreal forest composition and albedo

Permalink
https://escholarship.org/uc/item/9q3493hp

Journal
Global Change Biology, 17(9)

ISSN
1354-1013

Authors
BECK, PIETER SA
GOETZ, SCOTT J
MACK, MICHELLE C
et al.

Publication Date
2011-09-01

DOI
10.1111/j.1365-2486.2011.02412.x

Supplemental Material
https://escholarship.org/uc/item/9q3493hp#supplemental

Copyright Information
This work is made available under the terms of a Creative Commons Attribution License, availalbe at https://creativecommons.org/licenses/by/4.0/

Peer reviewed

eScholarship.org Powered by the California Digital Library
University of California

Global Change Biology

Global Change Biology (2011) **17**, 2853–2866, doi: 10.1111/j.1365-2486.2011.02412.x

The impacts and implications of an intensifying fire regime on Alaskan boreal forest composition and albedo

PIETER S. A. BECK*, SCOTT J. GOETZ*, MICHELLE C. MACK†, HEATHER D. ALEXANDER†, YUFANG JIN‡, JAMES T. RANDERSON‡ and M. M. LORANTY*

*Woods Hole Research Center, 149 Woods Hole Road, Falmouth, MA 02540, USA, †Department of Botany, University of Florida, 220 Bartram Hall, Gainesville, FL 32611-8526, USA, ‡Department of Earth System Science, University of California, Irvine, CA 92697, USA

Abstract

Climate warming and drying are modifying the fire dynamics of many boreal forests, moving them towards a regime with a higher frequency of extreme fire years characterized by large burns of high severity. Plot-scale studies indicate that increased burn severity favors the recruitment of deciduous trees in the initial years following fire. Consequently, a set of biophysical effects of burn severity on postfire boreal successional trajectories at decadal timescales have been hypothesized. Prominent among these are a greater cover of deciduous tree species in intermediately aged stands after more severe burning, with associated implications for carbon and energy balances. Here we investigate whether the current vegetation composition of interior Alaska supports this hypothesis. A chronosequence of six decades of vegetation regrowth following fire was created using a database of burn scars, an existing forest biomass map, and maps of albedo and the deciduous fraction of vegetation that we derived from Moderate Resolution Imaging Spectroradiometer (MODIS) satellite imagery. The deciduous fraction map depicted the proportion of aboveground biomass in deciduous vegetation, derived using a *RandomForest* algorithm trained with field data sets ($n = 69$, 71% variance explained). Analysis of the difference Normalized Burn Ratio, a remotely sensed index commonly used as an indicator of burn severity, indicated that burn size and ignition date can provide a proxy of burn severity for historical fires. LIDAR remote sensing and a bioclimatic model of evergreen forest distribution were used to further refine the stratification of the current landscape by burn severity. Our results show that since the 1950s, more severely burned areas in interior Alaska have produced a vegetation cohort that is characterized by greater deciduous biomass. We discuss the importance of this shift in vegetation composition due to climate-induced changes in fire severity for carbon sequestration in forest biomass and surface reflectance (albedo), among other feedbacks to climate.

Keywords: carbon storage, climate change, difference Normalized Burn Ratio (dNBR), feedback, Geoscience Laser Altimeter (GLAS), IceSat, Landsat, LIDAR, postfire succession

Received 23 August 2010 and accepted 24 January 2011

Introduction

Fire is a primary driver of long-term boreal forest dynamics including successional changes in vegetation composition (Viereck, 1973; Foote, 1983; Wurtz *et al*., 2006) and carbon cycling (Bond-Lamberty *et al*., 2007). In addition, fire generates an array of feedbacks between vegetation and climate, through combustion emissions during the fire event and through changes in carbon and energy exchange for decades afterwards due to fire impacts on soil moisture, temperature, drainage, decomposition, and vegetation composition (Chambers *et al*., 2005; Liu *et al*., 2005; Randerson *et al*., 2006). These feedbacks have the potential to modify northern hemisphere climate because the boreal biome is both expansive and dense in organic carbon, and because fire has substantial impacts on multiple forcing agents, including greenhouse gas fluxes, aerosols, black carbon deposition on snow and sea-ice, and surface albedo within burn perimeters (Bonan *et al*., 1995; Randerson *et al*., 2006).

The area of forest burned in Alaska has increased over the last four decades (Kasischke & Turetsky, 2006), and is projected to increase in the 21st century as a consequence of warming and drying during the fire season (Duffy *et al*., 2005; Balshi *et al*., 2009). The first, third, and seventh largest fire years since records began in the 1940s, were 2004, 2005, and 2009, respectively (Chapin *et al*., 2008; AICC, 2010). The annual area burned in Canada also shows an increasing trend during the second half of the 20th century (Gillett *et al*., 2004). Historical estimates from Russia are sparse (Conard *et al*., 2002) but recent fires have been anomalously large

Correspondence: Pieter S. A. Beck, tel. +1 508 444 1507, fax +1 508 444 1850, e-mail: pbeck@whrc.org

© 2011 Blackwell Publishing Ltd

(Kasischke *et al*., 2000; UNECE, FAO, GFMC, 2005; van der Werf *et al*., 2010), as have tundra fires recorded in Alaska (Jones *et al*., 2009). This intensification of the fire regime, with extreme fire years characterized by large burns becoming more frequent, has been attributed to climate warming (Gillett *et al*., 2004) and is expected to accelerate over the course of the 21st century. For example, combining historical relationships between weather-estimated fire danger and the annual area burned with projections from two global circulation models, Flannigan *et al*. (2005) estimated a 74–118% increase in area burned in Canada by the end of this century. More recently, estimates based on an empirical fire model for Alaska and Western Canada showed the average area burned per decade doubling by 2041–2050, relative to 1991–2000, and increasing on the order of 3.5–5.5 times by the end of the 21st century (Balshi *et al*., 2009).

The same drivers that cause greater areas to burn annually are also expected to increase burn severity (Stocks *et al*., 2000; Conard *et al*., 2002; Amiro *et al*., 2006), which is commonly defined as the proportion of organic matter consumed by fire (Keeley, 2009). In boreal forests, soils store most of the organic carbon; thus, burn severity is largely a function of the degree to which a fire consumes soil organic matter (Boby *et al*., 2010). Moreover, because in boreal North America most fires result in close to 100% tree mortality (Kasischke *et al*., 2006), burn severity and its effects on postfire soil conditions, including its physical properties and suitability for seed survival, initially regulate postfire vegetation communities (Johnstone & Chapin, 2006). The shallowness or absence of a porous, organic layer after severe burning reduces the likelihood of moisture stress affecting seedlings. In Alaska deciduous tree species benefit from a shallow postfire organic layer because they, in contrast to spruce trees, lack large reserves stored in seeds and a taproot to buffer against moisture stress (Schopmeyer, 1974; Kay, 1993). As a result, increased deciduous seedling recruitment and an ensuing dominance of tall shrubs and deciduous trees, particularly willow (*Salix* spp) and trembling aspen (*Populus tremuloides*) (hereafter simply aspen), tend to characterize severely burned landscapes in the first decade after fire (Johnstone & Kasischke, 2005; Johnstone *et al*., 2010b). In less severe burns, however, aspen are largely restricted to asexual resprouting (Viereck, 1973; Greene & Johnson, 1999) and evergreen seedlings have a higher recruitment success, relative abundance and persistence (Johnstone, 2005).

A similar pattern of high aspen recruitment in severely burned sites has been observed in other forested ecosystems of northwestern America such as Grand Teton and Yellowstone National Parks (Kay, 1993; Turner *et al*., 2003; Romme *et al*., 2005). In Yellowstone National Park, the intense ungulate browsing suppresses the growth of aspen seedlings in favor of coniferous trees such as lodgepole pine, preventing aspen trees from ever dominating the canopy except in areas where ungulate browsing is restricted (Turner *et al*., 2003). In interior Alaska, however, ungulates are unlikely to play a significant role in postfire succession because the region has a much lower density of ungulates: before wolf introduction in 1995, northern Yellowstone had 1.5–9 elk km^{-2} (White & Garrott, 2005), vs. 1–1.3 moose km^{-2} in a state-designated game management unit in interior Alaska (Wurtz *et al*., 2006).

Evidence suggests that in boreal forest of North America early postfire recruits, i.e. those that establish 3–6 years after fire, often dominate intermediate and mature boreal stand ages (Gutsell & Johnson, 2002; Johnstone *et al*., 2004). Yet specific differences in mortality can shift dominance patterns over a period of decades during regrowth (Gutsell & Johnson, 2002). The present ubiquity of spruce trees in interior Alaska despite the common presence of deciduous cohorts early in succession, for example, indicates that mortality of deciduous trees is higher than that of evergreen trees (Greene & Johnson, 1999; Yao *et al*., 2001). Despite this knowledge, there have been very few attempts to describe succession at decadal scales in response to boreal burn severity (Johnstone *et al*., 2004; Keane *et al*., 2004; Mack *et al*., 2008). This is due to the difficulty of measuring burn severity, particularly *post hoc* at the landscape level, and the paucity of long-term monitoring studies (see, however, Johnstone *et al*., 2004). Meanwhile, rates of biomass accumulation and the relative abundance of deciduous and evergreen species are pivotal to determining climate feedbacks associated with postfire succession (Viterbo & Betts, 1999; Lyons *et al*., 2008; Mack *et al*., 2008).

A range of legacy effects of burn severity on North American boreal forests have been hypothesized, with composition playing a central role in the direction and magnitude of productivity and albedo feedbacks to climate (Goetz *et al*., 2007; Mack *et al*., 2008). Where burning is severe, deciduous trees are expected to be more abundant for decades following fire disturbance. Since aspen, the dominant deciduous species in Alaska, generally show higher growth rates than black spruce (Yarie & Billings, 2002), more severely burned sites would accumulate biomass more quickly during intermediate stages of succession. Deciduous forests also have substantially higher albedo than evergreen forests, both during winter and summer (Amiro *et al*., 2006; Liu & Randerson, 2008; McMillan & Goulden, 2008) causing increased albedo with burn severity. Accumulation of soil organic carbon could change too because deciduous

vegetation produces more litter than does evergreen vegetation, although deciduous litter is generally more readily decomposed than evergreen litter and could potentially suppress moss growth (Johnstone *et al*., 2010a).

The balance of different climate forcing agents associated with a shift in vegetation composition will determine the net effect of the boreal fire regime on the climate system (Hinzman *et al*., 2003; Randerson *et al*., 2006; Euskirchen *et al*., 2009). Thus far, however, little empirical work has been done to quantify the impacts of burn severity on species composition at a landscape scale or to assess the associated feedbacks to climate. Here, we investigate whether vegetation patterns across the current Alaskan landscape reflect the expected legacy effects of burn severity over the past six decades. Specifically, we tested whether severely burned areas display higher deciduous cover, biomass, and albedo than less severely burned areas during intermediate stages of succession (10–50 years since fire). To do so, we relied on a chronosequence of current stands with ages, i.e. time since last fire, ranging from 10 to greater than 50 years, an existing biomass map (Blackard *et al*., 2008), and newly developed maps of deciduous cover and albedo.

Materials and methods

We describe (a) mapping of albedo and deciduous fraction of vegetation, which is defined as the percentage of aboveground biomass (AGB) stored in deciduous species, as derived from remote sensing data; (b) creation of a series of chronosequences reflecting biomass regrowth and albedo following fire; (c) stratification of burns in the study region (interior Alaska) into high- and low-severity burns; (d) assessment of the stratification approach, focusing on data uncertainty and potentially confounding covariates of burn severity. An overview of the main processing steps is given in Fig. 1.

Mapping albedo and deciduous fraction

Total short-wave albedo for spring and summer were calculated from Moderate Resolution Imaging Spectroradiometer (MODIS) Bidirectional Reflectance Distribution Function (BRDF) parameters (MCD43A1, Schaaf *et al*., 2002) at 500 resolution for the periods March 14–21 and July 28–August 4, respectively, using observations from the years 2004–2008 as input. We first calculated black sky albedo (BSA) at the mean solar zenith angle at 3 hourly intervals using the RossThick-LiSparse-Reciprocal model (Lucht *et al*., 2000) with MODIS total short-wave BRDF parameters, since the operational MODIS BRDF/Albedo products only provides BSA at local solar noon. Daily all sky albedo was then calculated as a sum

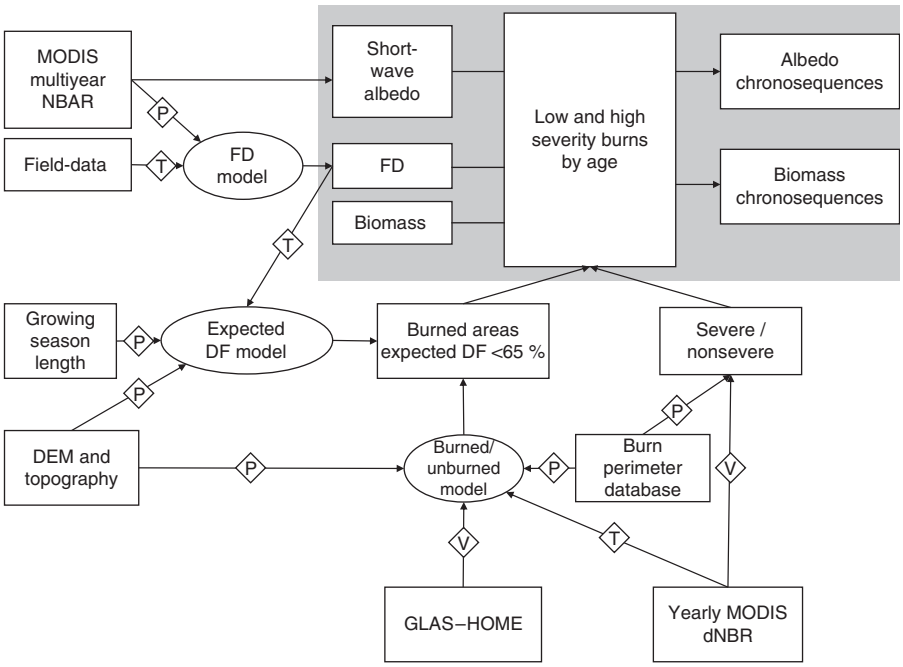

Fig. 1 Flowchart of data processing used to create chronosequences of biomass, deciduous fraction (FD), and short-wave albedo during postfire succession. Bold fonts indicate original data sets and oval boxes *RandomForest* models, with predictor variables indicated as ⟨P⟩, response variables used for model training as ⟨T⟩ and validation data as ⟨V⟩. MODIS, Moderate Resolution Imaging Spectroradiometer; NBAR, Nadir Bidirectional Reflectance Distribution Function Adjusted Reflectance; DEM, Digital Elevation Model; GLAS, Geoscience Laser Altimeter System; HOME, Height of Medium Energy; dNBR, difference Normalized Burn Ratio.

of 3 hourly BSA weighted by the ratio of 3 hourly direct incoming radiation over daily total incoming solar radiation plus white sky albedo weighted by the ratio of total daily diffuse radiation over total daily incoming solar radiation (Lewis & Barnsley, 1994). Radiation values were taken from the surface radiation budget data set provided by the World Climate Research Program/Global Energy and Water-Cycle Experiment (WCRP/GEWEX, Stackhouse *et al*., 2000).

The deciduous fraction (FD) of AGB was mapped using monthly composites of MODIS reflectance and field measurements using an ensemble regression tree model (Random Forest, Breiman, 2001). The field measurements of FD served as training data for the model and were collected in the summers of 2008 and 2009 in areas of homogenous vegetation cover that had not burned since 1987. The basal area of deciduous and evergreen trees and shrubs was measured in 269 plots measuring 10 and 20 m^2 and located along 100 m transects, with a maximum of 5 plots $transect^{-1}$. Using allometric equations, plot measurements were converted into deciduous and evergreen AGB from which FD was derived. Equations were produced from raw data available from the Bonanza Creek Long-Term Ecological Research Station (http://www.lter.uaf.edu/ascii/files/230_tree_biomass_data.csv) and augmented with those published by Yarie *et al*. (2007) and Bond-Lamberty *et al*. (2003). Plots were spread across 69 MODIS pixels, and data falling within identical MODIS pixels were grouped and regarded as single measurements in the analysis.

MODIS BRDF-adjusted reflectance data (NBAR, MCD43A4) from 2001 to 2008 were composited at 500 m spatial resolution to create monthly images of reflectance in seven spectral bands, based on the quality flags associated with the data (Baccini *et al*., 2008). Two data sets were created, one with data from different years processed separately, and one with data from the same month in different years pooled. The resulting images in the latter data set do not represent any changes in monthly reflectance since 2001, such as those due to disturbance or land cover, and were used to map FD. All band–month combinations between May and September, comprising 35 images in total, served as predictors in the *RandomForest* model calibrated using the field observations of FD. *RandomForest* models are ensembles of regression or classification trees, each using a bootstrap sample of the data where splits of the trees are determined by random subsets of the available predictors, randomly chosen at each node (Breiman, 2001). Furthermore, RandomForest is generally not likely to overfit the model to the data set used and can handle a large number of predictor variables, even when they are correlated, as is often the case with reflectance data. Crucially, performance metrics of *RandomForest*, such as the percentage of total variance in the reference observations explained by the model, are based on residuals associated with the data not included in the bootstrap sample used for calibration. Here, 500 trees with at least five observations in each terminal node comprised the *RandomForest* model. The predicted FD values were used to partition aboveground live forest biomass values mapped by Blackard *et al*. (2008) from a combination of MODIS, land cover, topography and climate images, into deciduous biomass (dBM) and evergreen biomass (eBM) in areas that burned between 1950 and 1991.

In addition to mapping FD in the 2001–2008 period, we also modeled the expected FD in absence of disturbance using growing season length (McKenney *et al*., 2006), permafrost extent (Jorgenson *et al*., 2008), geography and topography (elevation, slope, southern exposure, and wetness, Beven & Kirkby, 1979; Skidmore, 1989) as predictors in an environmental envelope model. In this case, FD values in 1600 uniformly distributed points in unburned areas (defined as areas more than 1 km but <10 km from any burns) served as training data for the *RandomForest* models.

Detecting burned areas

The database of Alaskan fire perimeters produced by the Bureau of Land Management, Alaska Fire Service (AFS), was acquired from the Alaska Geospatial Data Clearinghouse (http://agdc.usgs.gov/data/blm/fire) and used to define burns. Burn age was calculated with the year 2000 as reference, which is the start of the MODIS data record. Only burns between 10 and 50 years old were considered when constructing succession chronosequences to focus the study on intermediate stand ages (*sensu* Goetz *et al*., 2007; Mack *et al*., 2008), and to reduce effects of temporal uncertainty in the FD and albedo maps.

We focused our analysis on landscapes of interior Alaska that would normally be expected to follow a successional pathway ultimately leading from fire disturbance back to a black spruce forest, either directly or relayed via a deciduous phase. For the construction of the successional chronosequences, we excluded (i) fires that had burned areas smaller than 3200 ha, to minimize the effect of small patches in the landscape context and human-lit fires which are usually smaller than 500 ha in Alaska (DeWilde & Chapin, 2006); (ii) areas that were <1500 m from the burn perimeter, to reduce the effects of geographic misregistration in the database; (iii) areas that were <15 km from large roads or 7.5 km from smaller roads or the Alaska pipeline, to avoid effects of human disturbance and fire suppression activities, (iv) areas that had burned more than once since 1950 according to the fire database, to reduce effects of repeated burning, and (v) regions that had an expected FD $>65\%$, as predicted by the environmental envelope model, in order to reduce the influence of areas where vegetation succession was not expected to culminate in evergreen-dominated forests, such as alpine areas.

Stratifying burned areas by burn severity

Landscape-level estimates of burn severity have largely relied on changes (differences) in the Normalized Burn Ratio (dNBR, Lopez Garcia & Caselles, 1991) which is derived from a comparison of infrared reflectance in remotely sensed imagery of the growing season before and following fire events. The absence of such imagery historically renders the dNBR method unsuitable to retrospectively estimate burn severity before the Earth observation satellite era. Hence, we had to rely on nonremote sensing or retrospectively derived attributes of the burn scars to infer burn severity. In theory, burns that occur

later in the year are likely to be more severe since boreal soil dries out with time since snow melt and thus becomes more combustible (Kasischke & Johnstone, 2005). Analyses of *in situ* measured burn severity in five 2004 fires appear to confirm this pattern (Barrett *et al*., 2010). Combining this finding with the empirical evidence that the extent of a burn and its severity are modestly correlated (Duffy *et al*., 2007) and that the limited fire suppression in interior Alaska has a negligible effect on burn size in our study domain (DeWilde & Chapin, 2006), we hypothesized that large burns (>60 000 ha) that occur later in the year (after DOY 160) had higher levels of burn severity. These two criteria, burn timing and size, were then used to stratify all Alaskan burns since 1950 into low- and high-severity burns. The hypothesis underlying the stratification was tested using fires that occurred between 2002 and 2007 and for which July and August MODIS reflectance allowed us to map dNBR as a reference estimate of burn severity. To do this, NBR was mapped yearly from mean July–August reflectance values in MODIS band 2 (841–876 nm) and band 7 (2105–2155 nm) as NBR = (band 2−band 7)/(band 2 + band 7). dNBR for a fire in year t was then calculated as $NBR_{t+1}-NBR_{t-1}$.

The MODIS dNBR maps for the years 2002–2007 not only allowed us to test the burn severity stratification, but also to test the quality of the burn perimeter database. We tested (i) if the burn perimeters in the database contained remnant unburned areas, which would have to be excluded from analyses of postfire succession, (ii) whether the dNBR in 2002–2007 burns supported the proposed stratification into low- and high-severity burns based on burn size and timing, and (iii) if the burn severity stratification was correlated with landscape characteristics other than burn severity, which might bias patterns in successional trajectories. These three tests are described in more detail below.

Assessment of the burn severity stratification

The influence of unburned areas within burn perimeters. Any observations of successional changes in vegetation characteristics after fire are potentially sensitive to spatial inaccuracies in the burn perimeter database. Although spatial buffering of the perimeters can eliminate uncertainties regarding the exact location of the burn perimeter, it cannot account for the presence of unburned areas within the burn perimeters drafted by the AFS. There is evidence from Canada that the fraction of unburned area within burn perimeters increases with burn size (Eberhart & Woodard, 1987) and that unburned areas tend to have greater deciduous cover (Kafka *et al*., 2001). Including unburned areas in our analysis could thus bias our observations of successional vegetation changes and their dependency on burn severity, which we partly estimated from burn size. To avoid this, we first mapped unburned areas within burn perimeters where remote sensing data predating the fire were available. We then developed a model to retrospectively map potentially unburned areas in older burn perimeters in interior Alaska relying largely on the controls topography exerts over fire dynamics, primarily through soil moisture (Barrett *et al*., 2010).

Using the fire perimeter database, we quantified for each post-2001 burn polygon the fraction that might not have burned (i.e. unburned remnant forest patches), by mapping (a) the MODIS dNBR in each polygon and comparing it to (b) the MODIS dNBR of areas outside the burn polygon (>1500 and <5000 m from the burn perimeter and unburned since 1950). We then tagged as unburned the cells inside each burn perimeter where the dNBR was lower than the 95th percentile of the dNBR outside the burn (i.e. areas that were not significantly different from unburned areas). This allowed us to calculate for each burn since 2001 the unburned fraction within the burn perimeter. To assess the validity of this method for detecting unburned areas within the burn perimeters, we used light detection and ranging (LIDAR) data acquired by the Geoscience Laser Altimeter System (GLAS) onboard IceSat (Zwally *et al*., 2002). GLAS data are available since 2003 and are spatially discontinuous, with data recorded in 'shots' with a 65 m ellipsoidal footprint and spaced about 172 m apart along the overpass. GLAS data have previously been used to assess forest disturbance in Alaska (Goetz *et al*., 2010). We used the GLAS data here to derive estimates of vegetation height distribution (for GLAS processing stream, see Goetz *et al*., 2010). We used a GLAS metric that reflects the height at which half of the energy returned to the sensor is reached, commonly referred to as the Height of Medium Energy (HOME). HOME was used because we found it was less sensitive to algorithms designed to estimate canopy height by first detecting an initial return signal (from the top of the canopy) and then deconvolving a ground return (from the trailing edge of the LIDAR return). For the purpose of this study, we wanted to determine whether the distribution of HOME was lower in the year following fire than in the year before. Our assumption was that if HOME did not significantly change through time then it was unlikely that the location had experienced disturbance. In all, 12 622 GLAS measurements covering a total of 92 burns between 2004 and 2007 were processed to give pre- and postburn HOME estimates ($n_{\text{preburn}} = 5232$, $n_{\text{postburn}} = 7390$).

Once the unburned areas within the perimeters of post-2001 burns were mapped using dNBR, we characterized them by comparing their preburn land cover and their topography to that of the entire area within the burn perimeter. Land cover was estimated using a circa 2000 map at 0.01° spatial resolution [Global Land Cover (GLC) 2000, Bartholomé & Belward, 2005] reclassified into evergreen (GLC classes 4 and 11) vs. nonevergreen. The topographical variables southern exposure (Skidmore, 1989) and wetness [calculated as $\ln(\alpha/\tan\beta)$ where α is the local upslope area draining through a certain point per unit contour length and $\tan\beta$ is the local slope, Beven & Kirkby, 1979] were calculated from a digital elevation model and transformed to quantiles of their distribution within the burn. Statistical significance of the differences between unburned and burned areas was assessed within each burn perimeter using a χ^2-test for the evergreen fraction, and Wilcoxon's rank-sum tests for the other variables. Consistent patterns in the relative values of the topographical variables in unburned areas were then investigated across burn perimeters, by testing whether values were centered around 50%, for the quantiles, or 0%, for the differences in evergreen cover, using a Wilcoxon's signed-rank test. The aforementioned topographical parameters and the size of the burn were

used to develop a predictive classification model, using *RandomForest*, to retrospectively detect areas that were unlikely to have burned within all burn perimeters since 1950. Finally, we tested if there was a relationship between the fraction of unburned areas in a burn and its size, and if excluding areas that were modeled as unburned changed this relationship.

Comparison with dNBR

The validity of the burn severity stratification based on size and timing was tested using the dNBR. Because pre- and postfire remote sensing data are needed to calculate mean dNBR for a burn, only burns that occurred after 2001, and for which MODIS data were therefore available, were included in this test.

Covariates of burn size other than severity

After masking potentially unburned areas from burn perimeters since 1950 and prior to calculating chronosequences of regrowth after fire, we verified that the stratification of burn severity based on size and date of ignition did not introduce a bias in terms of topography (slope, southern exposure, and wetness) and bioclimate (growing season length and the expected deciduous fraction). If present, such a bias could influence the successional trajectories observed in low- and high-severity burns, independent of burn severity. To test for potential bias, both low- and high-severity burns were split into younger (<30 years) and older stands (>30 years), and a Kruskall–Wallis rank sum test applied to detect dissimilarities in topography and bioclimate between the different burn groups ($n_{\text{low severity, young}} = 125$, $n_{\text{high severity, young}} = 9$, $n_{\text{low severity, old}} = 93$, $n_{\text{high severity, old}} = 11$).

Results

We first describe the deciduous cover map we derived from MODIS remote sensing observations, then assess our approach used to estimate historical burn severity, and finally describe the chronosequences of biomass and albedo in response to burn severity.

Mapping deciduous fraction of vegetation

The deciduous fraction of the vegetation was robustly predicted by the *RandomForest* model using the MODIS reflectance image products (% variance explained = 71, $n = 69$, Fig. 2a). Spatial patterns in the resulting maps of FD clearly reflect the distribution of burn scars as well as non-disturbance-related ecotones, such as alpine belts and the boreal forest–tundra transition (Fig. 2a, b and d). The latter also are reflected by the map of expected FD in the absence of disturbance, predicted by a separate RF model (% variance explained = 54, $n = 1600$, Fig. 2c).

Assessment of the burn severity stratification

The influence of unburned areas within burn perimeters. We relied on a comparison of MODIS dNBR in- and outside burn perimeters to detect unburned areas within the burn perimeters, as recorded since 2001 in the AFS database (supporting information Fig. S1). An example is shown for the Boundary Fire in Fig. 3. The comparison of GLAS-derived canopy heights, and the HOME metric in particular, confirmed that the areas identified as unburned based on the MODIS dNBR undergo no detectable structural change (supporting information Fig. S2). Pre- and postburn GLAS-HOME values did not differ in unburned areas ($W = 47\,436$, $P = 0.55$, $n_{\text{preburn}} = 271$, $n_{\text{postburn}} = 336$), whereas they did in burned areas ($W = 15\,248\,949$, $P < 0.001$, $n_{\text{preburn}} = 5021$, $n_{\text{postburn}} = 7099$).

Unburned remnants within post-2001 burn perimeters tended to occupy more mesic areas than areas that burned (Fig. 4a, $V = 189$, $P < 0.001$, $n = 113$) and often had a relatively northerly topographic aspect (Fig. 4b, $V = 683$, $P = 0.06$, $n = 113$). In addition, unburned remnants tended to contain more deciduous vegetation before the fire than did areas that burned (Fig. 4c, $V = 458$, $P = 0.001$, $n = 113$). If these areas were not accounted for, observations of deciduous fraction during postfire succession would tend to be biased towards showing greater shifts from evergreen to deciduous cover.

While prefire vegetation cover can only be mapped if prefire remote sensing data are available, topographic wetness and exposure can be mapped for historical as well as recent fires. We exploited the effects that topographical wetness and topographical exposure have on the likelihood of burning to detect potentially unburned remnants since 1950. Using burns since 2001, where dNBR made it possible to distinguish between burned and unburned areas, we calibrated a *RandomForest* classification model to predict potentially unburned remnants within burn perimeters based on topographical variables, expressed as quantiles, and fire size.

The post-2001 burns that were classified as high severity based on their size and date of ignition, had a larger proportion of unburned areas within their perimeter, based on the dNBR, than those classified as low severity ($\text{mean}_{\text{high sev.}} = 7\%$, $\text{mean}_{\text{low sev.}} = 3\%$, $W = 726$, $P < 0.01$, $n_{\text{high sev.}} = 30$, $n_{\text{low sev.}} = 83$). Using the *RandomForest* classification algorithm to mask potentially unburned remnants these proportions and the difference between them were reduced ($\text{mean}_{\text{high sev.}} = 4\%$, $\text{mean}_{\text{low sev.}} = 2\%$, $W = 960$, $P = 0.03$, $n_{\text{high sev.}} = 30$, $n_{\text{low sev.}} = 83$). The algorithm used to mask unburned areas successfully detected 86% of the unburned areas in post-2001 burns. Yet, 74% of the area masked as unburned had actually burned. As a result, 15% of the

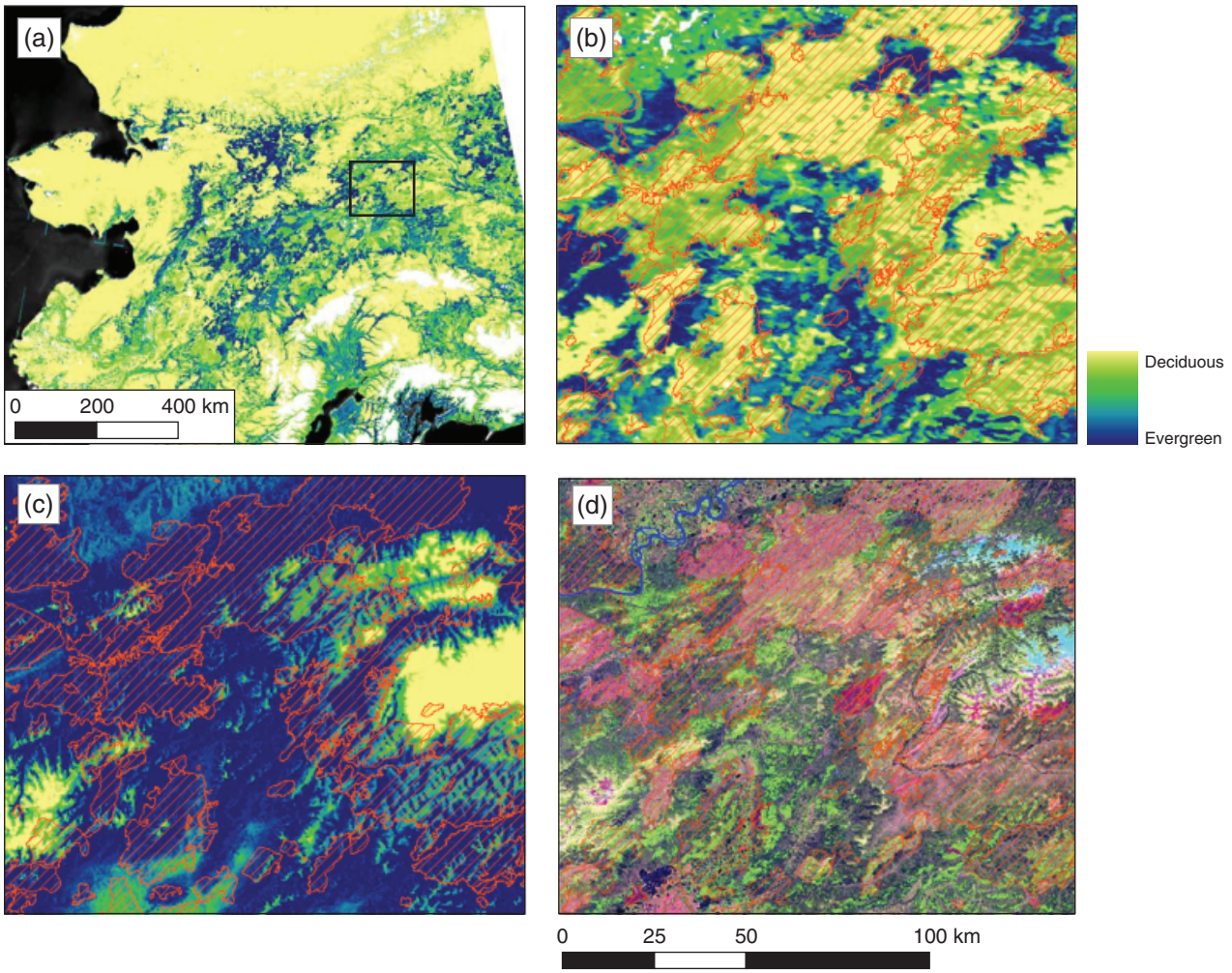

Fig. 2 (a, b) Deciduous fraction of vegetation in Central Alaska as mapped from MODIS NBAR reflectance. The black rectangle in (a) indicates the spatial domain of (b), (c), and (d), and orange hatched polygons indicate burn perimeters. (c) Expected deciduous fraction, in the absence of disturbance as predicted from bioclimate and topography. (d) A Landsat TM image (R-G-B = bands 5-4-3) acquired August 16, 2000. MODIS, Moderate Resolution Imaging Spectroradiometer; NBAR, Nadir Bidirectional Reflectance Distribution Function Adjusted Reflectance.

burned area appeared to have been unnecessarily excluded from our analysis of succession. This deliberate choice in the trade-off between the errors of omission and commission ensured that any effects of unburned areas on the successional patterns were minimized. In low- and high-severity burns after 2001, respectively, 5% and 8% of the area was mapped as unburned based on the dNBR, on average, and 14% and 22% was predicted as unburned by the *RandomForest* model.

Comparison with dNBR. Mean MODIS dNBR in the burns that were classified as high severity, based on their size and date of ignition, was not statistically significantly higher than in those classified as low severity, ($\text{mean}_{\text{high sev.}} = 0.38$, $\text{mean}_{\text{low sev.}} = 0.33$, Student's t-test: $t = -1.86$, $P = 0.06$, $n_{\text{high sev.}} = 26$, $n_{\text{low sev.}} = 87$) but were less likely to show a low dNBR, while some burns classified as low severity did show a low dNBR (Fig. 5).

Covariates of burn size other than severity. The criteria used to identify high severity burns in the database since 1950, i.e. larger than 60 000 ha and ignition date after DOY 160, did not introduce a topographical or bioclimatic bias. Younger and older high- and low-severity burns did not show a different distribution along gradients of topography ($P_{\text{slope}} = 0.52$, $P_{\text{exposure}} = 0.41$, $P_{\text{wetness}} = 0.07$), growing season length ($P = 0.06$), or expected deciduous fraction ($P = 0.33$, supporting information Fig. S3). Ultimately, the data selection described above retained 2.6 million ha for the construction of the chronosequences, of which 1.5 million ha were within

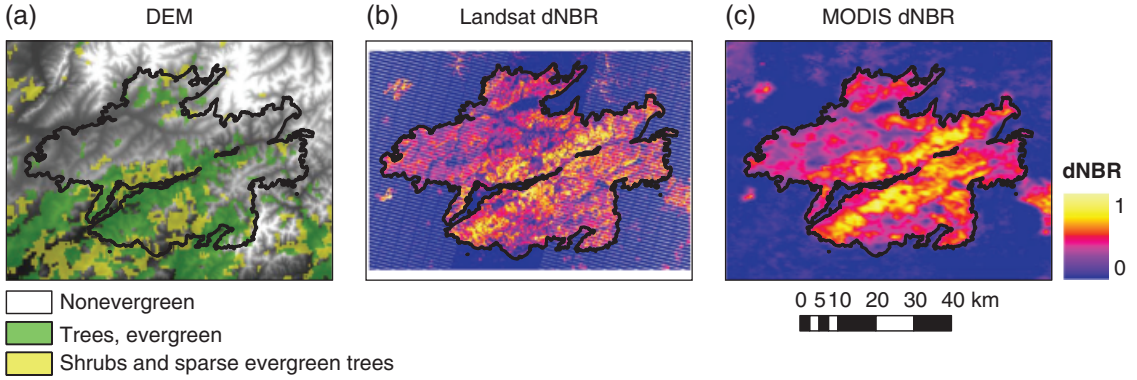

Fig. 3 Documented burn perimeter of the 2004 Boundary fire, overlaid on maps of preburn evergreen cover and a DEM (a), as well as dNBR derived from (b) Landsat (http://mtbs.gov, Eidenshink *et al*., 2007) and (c) MODIS data. The dNBR maps illustrate the existence of areas with very low dNBR, which might not have burned or have burned with minimal severity. DEM, Digital Elevation Model; dNBR, difference Normalized Burn Ratio; MODIS, Moderate Resolution Imaging Spectroradiometer.

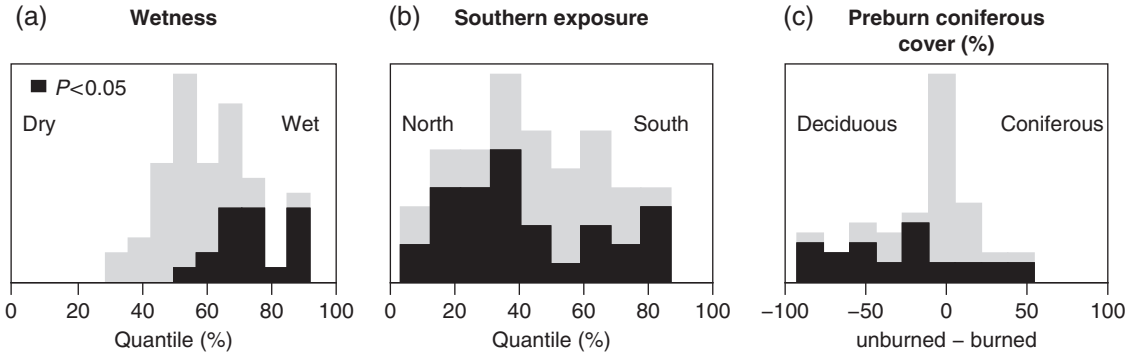

Fig. 4 (a) Histograms of topographical wetness and (b) southern exposure of unburned areas expressed as quantiles of the distribution within the entire burn perimeter, and (c) the mean difference in prefire coniferous cover (derived from GLC2000) of unburned and burned areas within the burn perimeters. Coniferous cover is calculated as the percentage of the total area that is classified as coniferous vegetation. A difference of −100 indicates that unburned areas were entirely covered by deciduous vegetation before the fire, whereas burned areas were entirely covered by coniferous vegetation. A difference of 100 indicates the opposite and a difference of 0 indicates that burned and unburned areas had an identical ratio of evergreen and deciduous cover before the fire. Black histogram sections indicate burn perimeters with statistically significant differences between burned and unburned areas based on a Wilcoxon's rank-sum test (a–b) or a χ^2-test (c), with $\alpha = 0.05$ for all tests. Grey sections indicate burn perimeters where differences are not statistically significant.

218 low-severity burns, and 1 million ha within 20 high-severity burns (supporting information Table S1).

Effects of burn severity on composition, biomass and albedo of regrowth

The deciduous fraction of vegetation in high severity burns was higher than in low-severity burns during the successional period considered here, i.e. from 10 to ~50 years after burning (Fig. 6). Deciduous vegetation-dominated biomass in the first 10–20 years of succession (mean DF = 75%, $n = 81$, $W = 3284$, $P < 0.001$, $H_1 = \mathrm{df} > 50\%$). In low-severity burns, dBM showed a steady decline after 25–30 years ($W = 4028$, $P < 0.001$, H_1: $\mathrm{dBM}_{<30\ \mathrm{years}} > \mathrm{dBM}_{\geq 30\ \mathrm{years}}$, $n_{<30\ \mathrm{years}} = 125$, $n_{>30\ \mathrm{years}} = 93$), whereas it increased in high-severity burns ($W = 80$, $P < 0.001$, H_1: $\mathrm{dBM}_{<30\ \mathrm{years}} < \mathrm{dBM}_{\geq 30\ \mathrm{years}}$, $n_{<30\ \mathrm{years}} = 9$, $n_{\geq 30\ \mathrm{years}} = 11$). At the same time, i.e. after 30 years or more, high-severity burns showed a greater total AGB than low-severity burns ($W = 665$, $P = 0.039$, H_1: $\mathrm{AGB}_{\mathrm{high\ sev.}} > \mathrm{AGB}_{\mathrm{low\ sev.}}$, $n_{\mathrm{high\ sev.}} = 11$, $n_{\mathrm{low\ sev.}} = 94$), in large part due to the difference in deciduous growth ($W = 729$, $P = 0.007$, H_1: $\mathrm{dBM}_{\mathrm{high\ sev.}} > \mathrm{dBM}_{\mathrm{low\ sev.}}$).

Boreal biomass estimates calculated from DBH measurements can vary by almost 100% depending on the parameterization of the allometric equations used in the calculation, even when these are species specific, and biomass density can vary greatly within stands (Mack *et al*., 2008). The forest biomass values reported here were extracted from a map by Blackard *et al*. (2008)

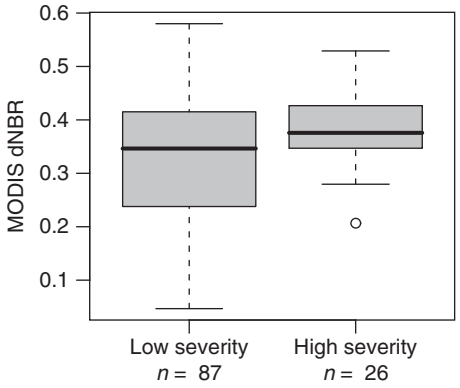

Fig. 5 Mean MODIS dNBR of burns after 2001, after excluding unburned areas, with high-severity burns defined as larger than 60 000 ha and starting after day 160 of the year. MODIS, Moderate Resolution Imaging Spectroradiometer; dNBR, difference Normalized Burn Ratio.

which covers the entire US and reportedly included live tree bole wood, stumps, branches, and twigs of trees 2.54 cm in diameter or larger. Biomass values in the ensuing chronosequences presented here (Fig. 6b and c) correspond relatively well with the original transect-level live biomass estimates measured in the field in stands of similar ages and used for the calculation of deciduous fractions [$12 \pm 3\,\mathrm{Mg\,ha^{-1}}$ (mean $\pm$ SE) in 22–30-year-old stands, $n = 13$, and $37 \pm 8\,\mathrm{Mg\,ha^{-1}}$ in 30–52-year-old stands, $n = 18$].

Because winter short-wave albedo was negatively correlated with evergreen fraction ($r = -0.71$, $P < 0.001$, df = 340), i.e. albedo was lower in more densely forested evergreen areas, it decreased with stand age in low-severity burns (Fig. 7). A similar but weaker pattern was observed in summer ($r = -0.55$, $P < 0.001$, df = 340). The higher deciduous fraction in high severity burns in all but the first decade after fire resulted in consistently higher summer albedo for at least four decades of succession ($W = 3702$, $P = 0.002$, H_1: $\mathrm{albedo}_{\mathrm{high\ sev.}} > \mathrm{albedo}_{\mathrm{low\ sev.}}$, $n_{\mathrm{high\ sev.}} = 20$, $n_{\mathrm{low\ sev.}} = 218$), which did not appear to decline with time ($W = 47$, $P = 0.72$, H_1: summer $\mathrm{albedo}_{<30\ \mathrm{years}} >$ summer $\mathrm{albedo}_{\geq 30\ \mathrm{years}}$, $n_{<30\ \mathrm{years}} = 9$, $n_{>30\ \mathrm{years}} = 11$). Differences between winter albedo in severe and nonsevere burns were apparent only after 20 years of succession ($W = 1357$, $P = 0.032$, H_1: winter $\mathrm{albedo}_{\mathrm{high\ sev.}} >$ winter $\mathrm{albedo}_{\mathrm{low\ sev.}}$, $n_{\mathrm{high\ sev.}} = 15$, $n_{\mathrm{low\ sev.}} = 142$).

Discussion

Post hoc *estimation of burn severity*

Our stratification of burns into low and high severity, based on their size and date of ignition, did not show a strong relationship with the dNBR of the burns. Burns in the high-severity stratum did have consistently high dNBR values, but so did some burns in the low-severity stratum (Fig. 5). This variability is not surprising because factors that operate at fine temporal and spatial scales are known to influence burn severity (Kasischke & Johnstone, 2005; Barrett *et al.*, 2010; Boby *et al.*, 2010). The ability of the dNBR

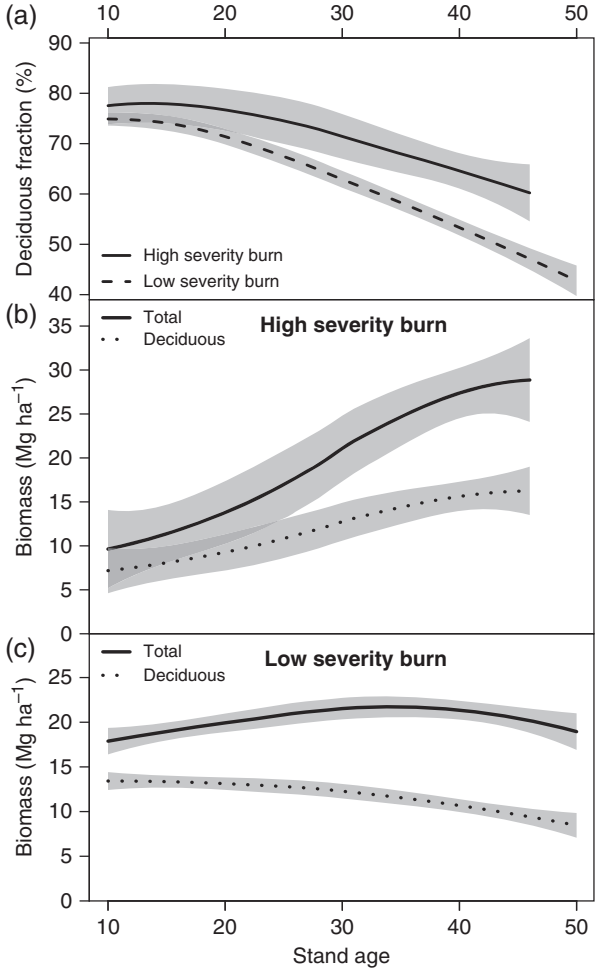

Fig. 6 (a) Deciduous fraction and total as well as deciduous aboveground biomass in (b) low- and (c) high-severity burns. Trajectories were calculated from a chronosequence of stands of different ages since burning, starting in 1950, which were stratified by burn severity estimated from the burn size and ignition date. Total biomass in (b) and (c) estimates are extracted from an existing map (Blackard *et al.*, 2008) and were partitioned into deciduous and evergreen biomass using the deciduous fraction mapped here from field data and 2001–2008 MODIS data. Lines are created through second order local polynomial regression fitting (span = 1.2, Cleveland *et al.*, 1992), where bold lines indicate the predicted mean and grey shading indicate estimated standard errors. MODIS, Moderate Resolution Imaging Spectroradiometer.

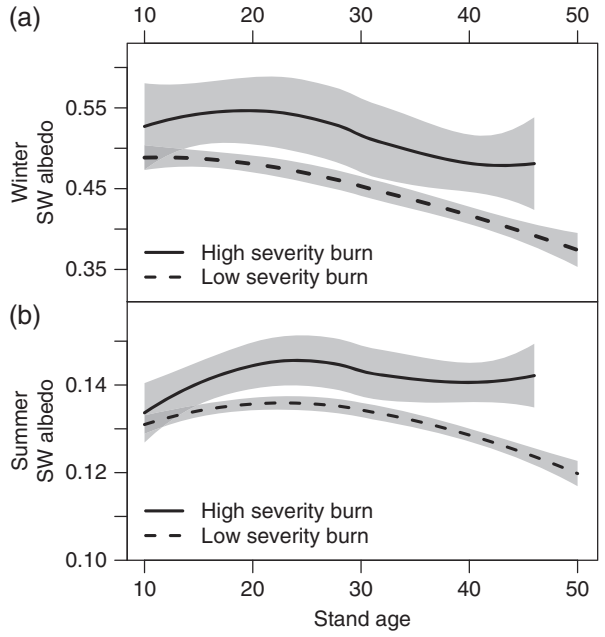

Fig. 7 Total short-wave albedo in (a) winter and (b) summer during regrowth in high- and low-severity burns since 1950. Winter and summer albedo were estimated from MODIS measurements during the periods March 14–21 and July 28–August 4, respectively, in 2004–2008. Lines are created through second order local polynomial regression fitting (span = 1.2, Cleveland *et al*., 1992), where bold lines indicate the predicted mean and grey shading indicate estimated standard errors. MODIS, Moderate Resolution Imaging Spectroradiometer.

to reflect burn severity in boreal regions is limited, however. While the dNBR is useful for distinguishing burned from unburned areas (Lopez Garcia & Caselles, 1991), it is disproportionately sensitive to changes in the vegetation canopy, which in turn limits its sensitivity to the bulk of the carbon consumed by fire in boreal regions, i.e. in the soil organic layer (Murphy *et al*., 2008; Barrett *et al*., 2010). In contrast, a recent field survey of 178 distinct Alaskan burns, showed how the depth of burning, which is correlated with burn severity, increased with both burn size and the timing of the fire in the season, supporting the stratification of burns into low and high severity used here (Turetsky *et al*., 2011).

The potential presence of severe burns in the low-severity stratum, in combination with our averaging of observations within a single burn, most probably attenuated the actual differences in succession between burn severity regimes. Moreover, because we pooled the MODIS data acquired over the 2001–2008 period, in order to calculate FD (see Materials and methods), we limited the sensitivity of our FD predictions to a ± 4 year time window. This might have further limited the distinction between FD in low- and high-severity burns, particularly in very young stands.

Succession-mediated legacy effects of burn severity

Over the 50-year period of regrowth considered here, greater burn severity promoted AGB accumulation as a result of shifting composition towards deciduous trees which typically have higher growth rates (Goetz & Prince, 1996; Mack *et al*., 2008). Over a longer time period, however, severely burned sites might have lower biomass due to lower spruce cover and self-thinning of dBM. The combination of more decomposable litter from deciduous trees, and a smaller input of relatively recalcitrant litter from evergreen trees, would also limit the buildup of organic carbon in the duff and soil layers in more severe burns, increasing the risk of permafrost degradation (Harden *et al*., 2006).

Over a period of decades, the radiative forcing associated with successional shifts in plant species composition can offset the forcing caused by greenhouse gas emissions released during the burning of mature spruce forests (Randerson *et al*., 2006). This is due primarily to an early succession deciduous vegetation phase that has considerably higher albedo during spring and summer than mature conifer forests (Chapin *et al*., 2000; Amiro *et al*., 2006; Lyons *et al*., 2008; McMillan & Goulden, 2008). An important question in this context is the degree to which higher burn severities (which would generate more carbon and aerosol emissions and more short-term positive forcing) might be balanced on decadal timescales by increases in the net primary production, stand density, and canopy cover of deciduous trees that have biophysical cooling properties.

Another important biophysical difference, for example, between boreal deciduous and evergreen vegetation involves rates of mid-summer canopy conductance and latent heat fluxes. Reported latent heat fluxes (evapotranspiration) in deciduous forests during summer are substantially higher than in coniferous stands, whereas sensible heat fluxes show an opposite pattern (Baldocchi *et al*., 2000; Eugster *et al*., 2000; Amiro *et al*., 2006; Liu & Randerson, 2008). Higher mid-summer evapotranspiration fluxes in deciduous stands may be linked with high rates of stomatal conductance and leaf-level evapotranspiration (Ewers *et al*., 2005; Bond-Lamberty *et al*., 2009), whereas latent energy fluxes in spruce forests, with their lower productivity and canopy conductance, may have a larger contribution of evaporation from the moss layer. These contrasting carbon and energy balance dynamics are currently not adequately characterized relative to burn severity in process-based ecosystem models (Bond-Lamberty *et al*., 2007; Euskirchen *et al*., 2009), despite their considerable

importance with respect to climate system feedbacks (McGuire *et al*., 2009).

Is boreal Alaska experiencing a biome shift?

The patterns of vegetation regrowth after fire in interior Alaska since 1950 indicate that severe burning promotes deciduous tree species for several decades. We expect the recent episodic fire years 2004, 2005 and 2009, in which a total of 5.7 million ha burned across the region ($\sim$ 5% of interior Alaska), to follow a similar trajectory. Extensive plot level field work in these burns supports this view (Johnstone *et al*., 2009). Directionality in the extent and severity of the fire regime and the consequences for postburn vegetation successional trajectories we documented here also support expectations of a shift towards a more deciduous-dominated landscape in Alaska in the near future (e.g. at least the next 50 years). These changes have implications not only for climate feedbacks, but also for game management and numerous other land management and resource uses of forest products in the region. We note that even in the absence of increased burn severity, a shortening of fire return interval will limit the development of mature spruce forests, increasing the presence of young deciduous vegetation (Johnstone *et al*., 2009).

Is this trend likely to continue in the future? Climate warming is projected to further intensify the fire regime, generating a higher frequency of extreme fire years characterized by large burns of high severity. At the same time, negative feedbacks from increasingly deciduous land cover have the potential to modify and mitigate future changes. Increasing the area burned annually will gradually reduce the amount of forest that has not recently burned across the landscape, and will reduce the mature conifer forest cover across interior Alaska. Deciduous forests that replace the fire adapted conifer-dominated stands are less likely to burn as a result of their architecture, lower flammability of tree tissues, and limited accumulation of fuels on the forest floor due to more rapid turnover of detritus (Dyrness *et al*., 1986; Hély *et al*., 2000; Krawchuk *et al*., 2006). This mechanism indicates increased deciduous cover may ultimately limit the intensification of the fire regime via a negative feedback effect, especially if warmer temperatures promote the longevity of deciduous trees.

The paleological record shows evidence of a strong black spruce-mediated biological control on the fire regime at centennial to millennial time scales: Between 6500 and 5600 years before present, following millennia when wildfires had been rare, black spruce expanded in interior Alaska, replacing less flammable vegetation communities dominated by birch, white spruce and alder (Lynch *et al*., 2003). This expansion of conifer-dominated vegetation appears to have been largely driven by an increased occurrence of wildfires resulting from, as well as promoting, increased black spruce cover, since there is no evidence of simultaneous climate change that would have intensified the fire regime (Lynch *et al*., 2004; Hu *et al*., 2006). However, the current climate in interior Alaska is moving beyond the optimal growth conditions for spruce growth (Beck *et al*., 2011) and is intensifying the fire regime at decadal timescales to the extent that it favors deciduous rather than evergreen regrowth, thus creating a negative feedback. Therefore, a new tipping point may be approaching where the boreal forest moves from evergreen dominance towards a greater cover of deciduous species. Such a biome shift would be accelerated by the other effects of ongoing climate change on spruce trees, such as drought stress (Barber *et al*., 2000; Beck *et al*., 2011) and increased susceptibility to pest outbreaks (Malmström & Raffa, 2000). Additional research on burn severity and its influence on vegetation succession in the boreal landscape is needed, particularly with respect to the magnitude and directionality of net feedbacks to climate and associated disturbance regimes.

Acknowledgements

The authors thank Alessandro Baccini and Mindy Sun for assistance with the MODIS reflectance and GLAS data processing, respectively, Glenn Juday for discussions on biome shifts and three anonymous reviewers for their valuable insights and constructive comments which improved the manuscript. We acknowledge support from NASA Ecosystems and Carbon Cycle Grant NNX08AG13G and NOAA Global Carbon Cycle Grant NA080AR4310526.

References

AICC (2010) *Yearly Alaska fire statistics*. Alaska Interagency Coordination Center. Available at http://fire.ak.blm.gov/predsvcs/intel.php (accessed 1 April 2010).

Amiro BD, Orchansky AL, Barr AG *et al*. (2006) The effect of post-fire stand age on the boreal forest energy balance. *Agricultural and Forest Meteorology*, **140**, 41–50.

Baccini A, Laporte N, Goetz SJ, Sun M, Dong H (2008) A first map of tropical Africa's above-ground biomass derived from satellite imagery. *Environmental Research Letters*, **3**, 045011, doi: 10.1088/1748-9326/3/4/045011.

Baldocchi D, Kelliher FM, Black TA, Jarvis PG (2000) Climate and vegetation controls on boreal zone energy exchange. *Global Change Biology*, **6**, 69–83.

Balshi MS, McGuire AD, Duffy P, Flanningan M, Walsh J, Mellilo J (2009) Assessing the response of area burned to changing climate in western boreal North America using a Multivariate Adaptive Regression Splines (MARS) approach. *Global Change Biology*, **15**, 578–600.

Barber VA, Juday GP, Finney BP (2000) Reduced growth of Alaskan white spruce in the twentieth century from temperature-induced drought stress. *Nature*, **406**, 668–673.

Barrett K, Kasischke ES, McGuire AD, Turetsky MR, Kane ES (2010) Modeling fire severity in black spruce stands in the Alaskan boreal forest using spectral and non-spectral geospatial data. *Remote Sensing of Environment*, **114**, 1494–1503.

Bartholomé E, Belward AS (2005) GLC2000: a new approach to global land cover mapping from earth observation data. *International Journal of Remote Sensing*, **26**, 1959–1977.

Beck PSA, Juday GP, Alix C *et al*. (2011) Changes in forest productivity across Alaska consistent with biome shift. *Ecology Letters*, doi: 10.1111/j.1461-0248.2011.01598.x.

Beven KJ, Kirkby MJ (1979) A physically based, variable contributing area model of basin hydrology. *Hydrological Sciences Bulletin*, **24**, 43–69.

Blackard JA, Finco MV, Helmer EH *et al*. (2008) Mapping U.S. forest biomass using nationwide forest inventory data and moderate resolution information. *Remote Sensing of Environment*, **112**, 1658–1677.

Boby LA, Schuur EAG, Mack MC, Verbyla D, Johnstone JF (2010) Quantifying fire severity, carbon, and nitrogen emissions in Alaska's boreal forest. *Ecological Applications*, **20**, 1633–1647.

Bonan GB, Chapin FS, Thompson SL (1995) Boreal forest and tundra ecosystems as components of the climate system. *Climate Change*, **29**, 145–167.

Bond-Lamberty B, Peckham SD, Ahl DE, Gower ST (2007) Fire as the dominant driver of central Canadian boreal forest carbon balance. *Nature*, **450**, 89–92.

Bond-Lamberty B, Peckham SD, Gower ST, Ewers BE (2009) Effects of fire on regional evapotranspiration in the central Canadian boreal forest. *Global Change Biology*, **15**, 1242–1254.

Bond-Lamberty B, Wang C, Gower ST (2003) Annual carbon flux from woody debris for a boreal black spruce fire chronosequence. *Journal of Geophysical Research*, **108**, 8220, doi: 10.1029/2001JD000839.

Breiman L (2001) Random forests. *Machine Learning*, **45**, 5–32.

Chambers SD, Beringer J, Randerson JT, Chapin FS III (2005) Fire effects on net radiation and energy partitioning: contrasting responses of tundra and boreal forest ecosystems. *Journal of Geophysical Research*, **110**, D09106, doi: 10.1029/2004jd005299.

Chapin FS, McGuire AD, Randerson J *et al*. (2000) Arctic and boreal ecosystems of western North America as components of the climate system. *Global Change Biology*, **6**, S211–S223.

Chapin FS, Trainor SF, Huntington O *et al*. (2008) Increasing wildfire in Alaska's boreal forest: pathways to potential solutions of a wicked problem. *BioScience*, **58**, 531–540.

Cleveland WS, Grosse E, Shyu WM (1992) Local regression models. In: *Statistical Models in S* (eds Chambers JM, Hastie TJ), pp. 309–376. Chapman & Hall, New York.

Conard SG, Sukhinin AI, Stocks BJ, Cahoon DR, Davidenko EP, Ivanova GA (2002) Determining effects of area burned and fire severity on carbon cycling and emissions in Siberia. *Climatic Change*, **55**, 197–211.

DeWilde L, Chapin FS (2006) Human impacts on the fire regime of Interior Alaska: interactions among fuels, ignition sources, and fire suppression. *Ecosystems*, **9**, 1342–1353.

Duffy PA, Epting J, Graham JM, Rupp TS, McGuire AD (2007) Analysis of Alaskan burn severity patterns using remotely sensed data. *International Journal of Wildland Fire*, **16**, 277–284.

Duffy PA, Walsh JE, Graham JM, Mann DH, Rupp TS (2005) Impacts of large-scale atmospheric-ocean variability on Alaskan fire season severity. *Ecological Applications*, **15**, 1317–1330.

Dyrness CT, Viereck LA, Van Cleve K (1986) Fire in taiga communities of interior Alaska. In: *Forest Ecosystems in the Alaskan Taiga: A Synthesis of Structure and Function* (eds Van Cleve K, Chapin FS, Flanagan PW, Viereck LA, Dyrness CT), pp. 74–86. Springer Verlag, New York.

Eberhart KE, Woodard PM (1987) Distribution of residual vegetation associated with large fires in Alberta. *Canadian Journal of Forest Research*, **17**, 1207–1212.

Eidenshink J, Schwind B, Brewer K, Zhu Z, Quayle B, Howard S (2007) A project for monitoring trends in burn severity. *Fire Ecology*, **3**, 3–21.

Eugster W, Rouse WR, Pielke RA *et al*. (2000) Land–atmosphere energy exchange in Arctic tundra and boreal forest: available data and feedbacks to climate. *Global Change Biology*, **6**, 84–115.

Euskirchen ES, McGuire AD, Rupp TS, Chapin FS, Walsh JE (2009) Projected changes in atmospheric heating due to changes in fire disturbance and the snow season in the western Arctic, 2003–2100. *Journal of Geophysical Research*, **114**, G04022, doi: 10.1029/2009jg001095.

Ewers BE, Gower ST, Bond-Lamberty B, Wang CK (2005) Effects of stand age and tree species on canopy transpiration and average stomatal conductance of boreal forests. *Plant, Cell and Environment*, **28**, 660–678.

Flannigan MD, Logan KA, Amiro BD, Skinner WR, Stocks BJ (2005) Future area burned in Canada. *Climate Change*, **72**, 1–16.

Foote MJ (1983) *Classification, description, and dynamics o f plant communities after fire in the taiga of interior Alaska*. Res. Pap. PNW-307, U.S. Department of Agriculture, Forest Service, Pacific Northwest Forest and Range Experiment Station.

Gillett NP, Weaver AJ, Zwiers FW, Flannigan MD (2004) Detecting the effect of climate change on Canadian forest fires. *Geophysical Research Letters*, **31**, L18211, doi: 10.1029/2004GL020876.

Goetz SJ, Mack MC, Gurney KR, Randerson JT, Houghton RA (2007) Ecosystem responses to recent climate change and fire disturbance at northern high latitudes: observations and model results contrasting northern Eurasia and North America. *Environmental Research Letters*, **2**, 045031, doi: 10.1088/1748-9326/2/4/045031.

Goetz SJ, Prince SD (1996) Remote sensing of primary production in boreal forest stands. *Agricultural and Forest Meteorology*, **78**, 149–179.

Goetz SJ, Sun M, Baccini A, Beck PSA (2010) Synergistic use of spaceborne LIDAR and optical imagery for assessing forest disturbance: an Alaska case study. *Journal of Geophysical Research*, **115**, G00E07, doi: 10.1029/2008jg000898.

Greene DF, Johnson EA (1999) Modelling recruitment of *Populus tremuloides, Pinus banksiana*, and *Picea mariana* following fire in the mixedwood boreal forest. *Canadian Journal of Forest Research*, **29**, 462–473.

Gutsell SL, Johnson EA (2002) Accurately ageing trees and examining their height-growth rates: implications for interpreting forest dynamics. *Journal of Ecology*, **90**, 153–166.

Harden JW, Manies KL, Turetsky MR, Neff JC (2006) Effects of wildfire and permafrost on soil organic matter and soil climate in interior Alaska. *Global Change Biology*, **12**, 2391–2403.

Hély C, Bergeron Y, Flannigan MD (2000) Effects of stand composition on fire hazard in mixed-wood Canadian boreal forest. *Journal of Vegetation Science*, **11**, 813–824.

Hinzman LD, Fukuda M, Sandberg DV, Chapin FS, Dash D (2003) FROSTFIRE: an experimental approach to predicting the climate feedbacks from the changing boreal fire regime. *Journal of Geophysical Research*, **108**, 8153, doi: 10.1029/2001JD000415.

Hu FS, Brubaker LB, Gavin DG, Higuera PE, Lynch JA, Rupp TS, Tinner W (2006) How climate and vegetation influence the fire regime of the Alaskan boreal biome: the Holocene perspective. *Mitigation and Adaptation Strategies for Global Change*, **11**, 829–846.

Johnstone J, Boby L, Tissier E, Mack M, Verbyla D, Walker X (2009) Postfire seed rain of black spruce, a semiserotinous conifer, in forests of interior Alaska. *Canadian Journal of Forest Research*, **39**, 1575–1588.

Johnstone J, Chapin F (2006) Effects of soil burn severity on post-fire tree recruitment in boreal forest. *Ecosystems*, **9**, 14–31.

Johnstone JF (2005) Effects of aspen (*Populus tremuloides*) sucker removal on postfire conifer regeneration in central Alaska. *Canadian Journal of Forest Research*, **35**, 483–486.

Johnstone JF, Chapin FS, Foote J, Kemmett S, Price K, Viereck LA (2004) Decadal observations of tree regeneration following fire in boreal forests. *Canadian Journal of Forest Research*, **34**, 267–273.

Johnstone JF, Chapin FS III, Hollingsworth TN, Mack MC, Romanovsky V, Turetsky MR (2010a) Fire, climate change, and forest resilience in interior Alaska. *Canadian Journal of Forest Research*, **40**, 1302–1312.

Johnstone JF, Hollingsworth TN, Chapin FS, Mack MC (2010b) Changes in fire regime break the legacy lock on successional trajectories in Alaskan boreal forest. *Global Change Biology*, **16**, 1281–1295.

Johnstone JF, Kasischke ES (2005) Stand-level effects of soil burn severity on postfire regeneration in a recently burned black spruce forest. *Canadian Journal of Forest Research*, **35**, 2151–2163.

Jones BM, Kolden CA, Jandt R, Abatzoglou JT, Urban F, Arp CD (2009) Fire behavior, weather, and burn severity of the 2007 Anaktuvuk River Tundra fire, North Slope, Alaska. *Arctic, Antarctic, and Alpine Research*, **41**, 309–316.

Jorgenson MT, Yoshikawa K, Kanveskiy M *et al*. (2008) Permafrost characteristics of Alaska. In: *Proceedings of the Ninth International Conference on Permafrost* (eds Kane D, Hinkle K), pp. 121–122. University of Alaska, Fairbanks, AK.

Kafka V, Gauthier S, Bergeron Y (2001) Fire impacts and crowning in the boreal forest: study of a large wildfire in western Quebec. *International Journal of Wildland Fire*, **10**, 119–127.

Kasischke ES, French NHF, O'Neill KP, Richter DD, Bourgeau-Chavez LL, Harrell PA (2000) Influence of fire on long-term patterns of forest succession in Alaskan boreal forests. In *Fire, Climate Change, and Carbon Cycling in the Boreal Forest* (eds Kasischke ES, Stocks BJ), pp. 214–238. Springer, Berlin.

Kasischke ES, Johnstone JF (2005) Variation in postfire organic layer thickness in a black spruce forest complex in interior Alaska and its effects on soil temperature and moisture. *Canadian Journal of Forest Research*, **35**, 2164–2177.

Kasischke ES, Rupp TS, Verbyla DL (2006) Fire trends in the Alaskan boreal forest. In: *Alaska's Changing Boreal Forest* (eds Chapin FS III, Oswood MW, Van Cleve K, Viereck LA, Verbyla DL), pp. 285–301. Oxford University Press, New York.

Kasischke ES, Turetsky MR (2006) Recent changes in the fire regime across the North American boreal region – spatial and temporal patterns of burning across Canada and Alaska. *Geophysical Research Letters*, **33**, L09703, doi: 10.1029/2006GL025677.

Kay CE (1993) Aspen seedlings in recently burned areas of Grand Teton and Yellowstone National Parks. *Northwest Science*, **67**, 94–104.

Keane RE, Cary GJ, Davies ID *et al*. (2004) A classification of landscape fire succession models: spatial simulations of fire and vegetation dynamics. *Ecological Modelling*, **179**, 3–27.

Keeley JE (2009) Fire intensity, fire severity and burn severity: a brief review and suggested usage. *International Journal of Wildland Fire*, **18**, 116–126.

Krawchuk MA, Cumming SG, Flannigan MD, Wein RW (2006) Biotic and abiotic regulation of lightning fire initiation in the mixedwood boreal forest. *Ecology*, **87**, 458–468.

Lewis P, Barnsley MJ (1994) *Influence of the sky radiance distribution on various formulations of the earth surface albedo*. Proceedings of the Sixth International Symposium on Physical Measurements and Signatures in Remote Sensing, Val d'Isere, France, pp. 707–715.

Liu H, Randerson JT (2008) Interannual variability of surface energy exchange depends on stand age in a boreal forest fire chronosequence. *Journal of Geophysical Research*, **113**, G01006, doi: 10.1029/2007JG000483.

Liu H, Randerson JT, Lindfors J, Chapin FS III (2005) Changes in the surface energy budget after fire in boreal ecosystems of interior Alaska: an annual perspective. *Journal of Geophysical Research*, **110**, D13101, doi: 10.1029/2004jd005158.

Lopez Garcia MJ, Caselles V (1991) Mapping burns and natural reforestation using Thematic Mapper data. *Geocarta International*, **1**, 31–37.

Lucht W, Schaaf CB, Strahler AH (2000) An algorithm for the retrieval of albedo from space using semiempirical BRDF models. *IEEE Transactions on Geoscience and Remote Sensing*, **38**, 977–998.

Lynch JA, Clark JS, Bigelow NH, Edwards ME, Finney BP (2003) Geographical and temporal variations in fire history in boreal ecosystems in Alaska. *Journal of Geophysical Research-Atmospheres*, **108**, 8152, doi: 10.1029/2001JD000332.

Lynch JA, Hollis JL, Hu FS (2004) Climatic and landscape controls of the boreal forest fire regime: Holocene records from Alaska. *Journal of Ecology*, **92**, 477–489.

Lyons EA, Jin Y, Randerson JT (2008) Changes in surface albedo after fire in boreal forest ecosystems of interior Alaska assessed using MODIS satellite observations. *Journal of Geophysical Research*, **113**, G02012, doi: 10.1029/2007JG000606.

Mack M, Treseder K, Manies K *et al*. (2008) Recovery of aboveground plant biomass and productivity after fire in mesic and dry black spruce forests of interior Alaska. *Ecosystems*, **11**, 209–225.

Malmström CM, Raffa KF (2000) Biotic disturbance agents in the boreal forest: considerations for vegetation change models. *Global Change Biology*, **6**, 35–48.

McGuire AD, Anderson LG, Christensen TR *et al*. (2009) Sensitivity of the carbon cycle in the Arctic to climate change. *Ecological Monographs*, **79**, 523–555.

McKenney DW, Pedlar JH, Papadopol P, Hutchinson MF (2006) The development of 1901–2000 historical monthly climate models for Canada and the United States. *Agricultural and Forest Meteorology*, **138**, 69–81.

McMillan AMS, Goulden ML (2008) Age-dependent variations in the biophysical properties of boreal forests. *Global Biogeochemical Cycles*, **22**, GB2019, doi: 10.1029/2007GB003038.

Murphy KA, Reynolds JH, Koltun JM (2008) Evaluating the ability of the differenced Normalized Burn Ratio (dNBR) to predict ecologically significant burn severity in Alaskan boreal forests. *International Journal of Wildland Fire*, **17**, 490–499.

Randerson JT, Liu H, Flanner MG *et al*. (2006) The impact of boreal forest fire on climate warming. *Science*, **314**, 1130–1132.

Romme WH, Turner MG, Tuskan GA, Reed RA (2005) Establishment, persistence, and growth of aspen (*Populus tremuloides*) seedlings in Yellowstone National Park. *Ecology*, **86**, 404–418.

Schaaf CB, Gao F, Strahler AH *et al*. (2002) First operational BRDF, albedo nadir reflectance products from MODIS. *Remote Sensing of Environment*, **83**, 135–148.

Schopmeyer CS (1974) *Seeds of Woody Plants in the United States*. United States Department of Agriculture Forest Service, Washington, DC, USA.

Skidmore AK (1989) A comparison of techniques for calculating gradient and aspect from a gridded digital elevation model. *International Journal of Remote Sensing*, **3**, 323–334.

Stackhouse PW, Gupta SK, Cox SJ, Chiacchio M, Mikovitz JC (2000) The WCRP/GEWEX Surface Radiation Budget Project Release 2: an assessment of surface fluxes at 1 degree resolution. In: *IRS 2000: Current Problems in Atmospheric Radiation* (eds Smith WL, Timofeyev YM), pp. 24–29. International Radiation Symposium, St. Petersburg, Russia.

Stocks BJ, Fosberg MA, Wotton BM, Lynham TJ, Ryan KC (2000) Climate change and forest fire activity in North American boreal forests. In: *Fire, Climate Change, and Carbon Cycling in the Boreal Forest* (eds Kasischke ES, Stocks BJ), pp. 368–376. Springer, New York.

Turetsky MR, Kane ES, Harden JW, Ottmar RD, Manies KL, Hoy E, Kasischke ES (2011) Recent acceleration of biomass burning and carbon losses in Alaskan forests and peatlands. *Nature Geoscience*, **4**, 27–31.

Turner MG, Romme WH, Tinker DB (2003) Surprises and lessons from the 1988 Yellowstone fires. *Frontiers in Ecology and the Environment*, **1**, 351–358.

UNECE, FAO, GFMC (2005) Special issue on Russia. In: *International Forest Fire News*, Vol. 32 (ed. Goldammer JG). United Nations Publications, New York, 131pp.

van der Werf GR, Randerson JT, Giglio L *et al*. (2010) Global fire emissions and the contribution of deforestation, savanna, forest, agricultural and peat fires (1997–2009). *Atmospheric Chemistry and Physics Discussions*, **10**, 16153–16230.

Viereck LA (1973) Wildfire in the taiga of Alaska. *Quaternary Research*, **3**, 465–495.

Viterbo P, Betts AK (1999) Impact on ECMWF forecasts of changes to the albedo of the boreal forests in the presence of snow. *Journal of Geophysical Research*, **104**, 27803–27810.

White PJ, Garrott RA (2005) Yellowstone's ungulates after wolves – expectations, realizations, and predictions. *Biological Conservation*, **125**, 141–152.

Wurtz TL, Ott RA, Maisch JC (2006) Timber harvest in interior Alaska. In: *Alaska's Changing Boreal Forest* (eds Chapin FS III, Oswood MW, Van Cleve K, Viereck LA, Verbyla DL), pp. 302–308. Oxford University Press, New York.

Yao X, Titus SJ, MacDonald A (2001) A generalized logistic model of individual tree mortality for aspen, white spruce, and lodgepole pine in Alberta mixedwood forests. *Canadian Journal of Forest Research*, **31**, 283–291.

Yarie J, Billings S (2002) Carbon balance of the taiga forest within Alaska: present and future. *Canadian Journal of Forest Research*, **32**, 757–767.

Yarie J, Kane E, Mack MC (2007) Aboveground biomass equations for the trees of interior Alaska. *AFES Bulletin*, **115**, 1–16.

Zwally HJ, Schutz B, Abdalati W *et al*. (2002) ICESat's laser measurements of polar ice, atmosphere, ocean, and land. *Journal of Geodynamics*, **34**, 405–445.

Supporting Information

Additional Supporting Information may be found in the online version of this article:

Figure S1. (a) The 95th percentile of the Moderate Resolution Imaging Spectroradiometer (MODIS) difference Normalized Burn Index (dNBR) observed in an unburned area around fire polygons (>1500 m and <5000 m from the burn perimeter and unburned since 1950) was used to screen the fire polygons as registered in a database of Alaskan fires produced by the Bureau of Land Management, Alaska Fire Service (AFS). For areas that burned between 2002 and 2007, areas within the fire polygon that had a dNBR below this associated threshold dNBR value were marked as potentially unburned. b) This screening resulted in an increase of the mean dNBR of the burned areas and c) a reduction in the size of the areas considered burned. Only burns where sets of at least 100 (500 m) MODIS pixels were available to determine the threshold (unburned) dNBR value and the mean dNBR in the burned area are included in the plots.

Figure S2. Distribution of vegetation heights as quantified by the Height of Medium Energy (HOME) recorded by the Geoscience Laser Altimeter System (GLAS) onboared Icesat. Height distributions are shown before (grey shading) and after (black lines) fire events in areas marked as a) unburned and b) burned inside the burn perimeters registered in a database of Alaskan fires produced by the Bureau of Land Management, Alaska Fire Service (AFS). Unburned areas were distinguished from burned areas based on the comparison of the difference Normalized Burn Ratio (dNBR) recorded by the Moderate Resolution Imaging Spectroradiometer (MODIS) inside and outside the fire polygons.

Figure S3. Topographic slope, exposure, and wetness, meteorological growing season length and the expected deciduous fraction predicted by a bioclimatic envelope model for low severity (LS) and high severity (HS) burns, that are younger and older than 30 years (labelled as young and old, respectively, LS-young: $n = 124$; LS-old: $n = 94$; HS-young: $n = 9$; HS-old: $n = 11$).

Table S1. Names, sizes and year of burning as registered in a database of Alaskan fires produced by the Bureau of Land Management, Alaska Fire Service (AFS), of the fires classified here as 'high severity' in the creation of deciduous and evergreen biomass chronosequences.

Please note: Wiley-Blackwell is not responsible for the content or functionality of any supporting materials supplied by the authors. Any queries (other than missing material) should be directed to the corresponding author for the article.